Formation of N^{13} in High-Energy Nuclear Reactions*

I. DOSTROVSKY
The Weizmann Institute of Science, Rehovoth, Israel and Chemistry Department, Brookhaven National Laboratory, Upton, New York,

Z. FRAENKEL
The Weizmann Institute of Science, Rehovoth, Israel,

AND

J. HUDIS
Chemistry Department, Brookhaven National Laboratory, Upton, New York

(Received April 10, 1961)

Experimental cross sections are reported for the formation of N^{13} in the bombardment of Zn, In, Pb, and *U* with protons of 1.0, 1.9, and 2.9 Bev energy. These values are compared with theoretical N^{13} emission cross sections for protons energies of 0.84 and 1.84 Bev. The calculations are based on the evaporation model. The previously described Monte Carlo procedure was modified in order to obtain better statistical accuracy for the calculated N^{13} cross sections. Previously computed emission cross sections for He^6, Li^8, and Be^7 were also recomputed using the modified Monte Carlo procedure. The cross sections were computed for three different formulations of the interaction radius. Good fit with the experimental He^6, Li^8, and Be^7 cross sections is obtained when the smaller values for the interaction radius are used. However, the fit with the experimental N^{13} values is not good enough to exclude processes other than evaporation as contributing to the experimentally observed cross sections.

I. INTRODUCTION

THE formation cross sections of N^{13} resulting from the interaction of high-energy protons and various targets have been determined. Although similar experimental results have been reported on the yields of other light nuclides in this mass region[1–4] it was thought desirable to investigate the specific case of N^{13} in order to shed further light on the mechanism of light-nuclide production in high-energy nuclear reactions.

It has been suggested [1,3,5] that the yields of light nuclides such as He^6, Be^7, and Li^8 may be explained by an evaporation mechanism in which not only neutrons, protons, alpha particles, but also these heavy particles are boiled out of the highly excited nuclei resulting from the interaction of high-energy protons with heavy target atoms. Detailed evaporation calculations[5,6] have shown this approach to be surprisingly successful. In order to see just how far it may be extended it is obviously necessary to compare observed formation cross sections with theoretical predictions for the yields of heavier evaporated particles. One difficulty with the calculation is that it must be performed not only for the emission of each particle in its ground state but also for the possibility of its emission in any of its bound excited states, with appropriate statistical weights given to each state. Therefore, if one wishes to calculate the evaporation probability of a particular heavy particle, all of its bound excited states and their spins must be known. For nuclei with $A>10$, complete data of this type are generally not available, and calculated evaporation probabilities are therefore subject to large uncertainties. In this respect, N^{13}, with no particle-stable excited states is unique, and is the obvious choice for comparison between experiment and theory. The formation cross section of N^{13} from Zn, In, Pb, and U targets were determined at incident proton energies of 1.0, 1.9, and 2.9 Bev. The calculated emission probabilities of N^{13} from the same targets at incident proton energy of 940 and 1840 Mev have been obtained using the Monte Carlo procedure described previously.[6] It was found, however, that in order to obtain reasonable statistical accuracy of the calculated cross sections the calculation had to be modified to handle very rare events. The modified calculation is described in Sec. VII. With the availability of a computer program which yields improved statistical results in the emission probabilities of heavy particles, the calculated cross sections for the evaporation of He^6, Li^8, and Be^7 were redetermined and are discussed in Sec. VIII.

II. TARGETS AND IRRADIATIONS

Pure foils of zinc ($\sim$70 mg/cm^2), indium ($\sim$36 mg/cm^2), lead ($\sim$100 mg/cm^2), and uranium ($\sim$100 mg/cm^2) were irradiated in the circulating beam of the Cosmotron. Each target consisted of a one-mil aluminum monitor foil, a guard foil to prevent recoiling N^{13} atoms produced in the monitor foil from entering the target foil, and the target foil itself. For zinc targets an additional 70-mg/cm^2 zinc foil was used as the guard foil. One-mil silver was used as the guard foil in the indium targets and $\frac{1}{2}$-mil gold was used with lead and uranium targets. The irradiations were of

* Research supported in part by the U. S. Atomic Energy Commission.

[1] F. S. Rowland and R. L. Wolfgang, Phys. Rev. **110**, 175 (1958).
[2] E. Baker, G. Friedlander, and J. Hudis, Phys. Rev. **112**, 1319 (1958).
[3] S. Katcoff, Phys. Rev. **114**, 905 (1959).
[4] R. A. Sharp (private communication on C^{11} yields).
[5] J. Hudis and J. M. Miller, Phys. Rev. **112**, 1322 (1958).
[6] I. Dostrovsky, Z. Fraenkel, and P. Rabinowitz, Phys. Rev. **118**, 791 (1960).

10-min duration at a beam intensity of between 10^9 and 10^{10} protons/sec. The details of the irradiation procedure have been described previously.[7] Absolute cross sections were based on the value of 10.8 mb for the $Al^{27}(p,3pn)Na^{24}$ monitor reaction between 1 and 3 Bev.[8]

III. CHEMICAL PROCEDURE

Since N^{13} has a 10-min half-life, the chemical separation had to be fast; in addition, of course, it had to meet the usual requirements of good yield and good decontamination from other activities and it had to ensure complete isotopic mixing between the radioactive nitrogen aroms formed during the irradiation and the inactive carrier atoms added during the separation procedure. The possibility existed that after the targets were dissolved the nitrogen atoms formed could be in any or all of the possible oxidation states ranging from 3− to 5+. A separation procedure was devised to recover nitrogen quickly regardless of its initial oxidation state. Figure 1 is a diagram of the apparatus used for this purpose.

After irradiation the target foils were dissolved in flask A (see Appendix for details of target solution) by addition of the appropriate acid plus NH_4^+ ion carrier, and any gases liberated were swept through the line with a mixture of He and CH_4 bypassing collection flask C. The function of furnaces $F1$ and $F2$ was to convert any gaseous carbon compound to CO_2, which was then removed from the gas stream by trap $T2$. Any H_2 evolved during the dissolution of the target was converted to H_2O in $F1$ and frozen out in $T1$. Only N_2, N_2O, and rare gases should come through the line. The molten Li trap then effectively stripped N_2 and N_2O away from the rare gases. Any rare-gas activity produced in the irradiation was then trapped on charcoal at −190°C.

The individual components of the system were checked in separate experiments using N^{13} tracer produced by fast-neutron irradiation of NH_4NO_3 to ascertain that each part of the apparatus functioned as expected. Special precautions were taken in checking the efficiency of the molten Li trap for removing the nitrogen gases from a helium stream, and efficiencies of >90% were observed.

After the target was completely dissolved, He and CH_4 sweeping was continued for about one minute. 10N NaOH was added to flask A through a hypodermic syringe, and the basic target solution was then boiled to distill NH_3 through flask B, containing 1N NaOH and $KMnO_4$, into collection flask C in which saturated boric acid was present to trap NH_3. The $KMnO_4$ was present to oxidize any volatile impurities such as AsH_3, SbH_3, etc. Flask C also contained an amount of HCl

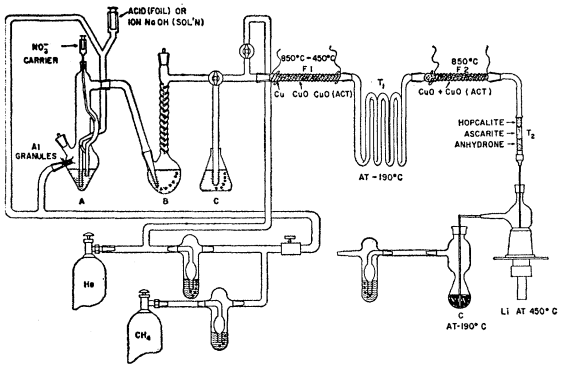

FIG. 1. Experimental apparatus.

which was equivalent to ~85% yield of NH_3, plus brom cresol purple indicator. The NH_3 distillation was continued until the indicator changed color and then perhaps for an additional minute.

After the original NH_3 fraction had been collected, nitrate ion carrier was added to the target solution and reduced to NH_3 by the addition of aluminum granules. The reaction rate was controlled initially by cooling and later by heating to maintain a very vigorous but controllable reaction, which was essential to obtain high yields. The NH_3 formed was distilled and collected in a fresh collection flask C^1 in the manner previously discussed.

The three nitrogen fractions, N_2 and N_2O in the Li trap, NH_4^+ in flask C, and NO_3^- in flask C^1 were all counted. For all target materials studied, when dissolved as described in the Appendix, all of the N^{13} activity was found to be in the original NH_4^+ fraction. This fortunate circumstance, once proven for each target material, allowed the use of a much faster separation process. Targets were dissolved in centrifuge tubes containing the appropriate acid plus NH_4^+ carrier, boiled to expel gases, and then transferred to flask A. NaOH was added and NH_3 distilled to flask B containing 1N NaOH and $KMnO_4$ at 0°C, where the NH_3 was trapped. The trapping was shown to be quite effective since during this operation, flask C contained saturated boric acid plus indicator and in no run was any color change observed. After a few minutes distillation, flask C was replaced by boric acid plus HCl equivalent to ~85% chemical yield and flask B was heated to boil out the NH_3. This NH_3 fraction in H_3BO_3 was transferred to a clean distillation flask, made basic with 10N NaOH and NH_3 redistilled and collected in the same fashion. The product from the third NH_3 distillation was then counted. Chemical yields were ~85% and the entire separation required only about 10 min.

IV. ACTIVITY MEASUREMENTS

The N^{13} activity was detected by placing the flasks containing the purified nitrogen as $N^{13}H_3$ trapped in saturated boric acid directly on top of a 2-in.×2-in.

[7] G. Friedlander, J. Hudis, and R. L. Wolfgang, Phys. Rev. **99**, 263 (1955).
[8] J. B. Cumming, G. Friedlander, and C. Swartz, Phys. Rev. **111**, 1386 (1958).

TABLE I. Experimental and calculated cross sections (in mb) for the formation of He^6, Li^8, Be^7 and N^{13} from various targets.

Target[a]	Light nuclide	940 Mev Experimental	940 Mev Calculated Eq. (7)[b]	940 Mev Calculated Eq. (8)	940 Mev Calculated Eq. (9)	1840 Mev Experimental	1840 Mev Calculated Eq. (7)[b]	1840 Mev Calculated Eq. (8)	1840 Mev Calculated Eq. (9)	2.9 Bev Experimental
Cu	He^6 [c]	2±1	3.29	1.83	3.56	4±2	6.73	4.10	9.01	
	Li^8 [d]					3	3.97	2.26	4.72	
	Be^7 [e]	4.4±1.1	6.06	2.80	3.66	11.7±2.9	13.52	7.56	6.45	
Zn	N^{13} [f]	0.13	0.085	0.028	0.029	0.33	0.157	0.079	0.056	0.51
Ag	He^6 [c]	4±2	6.66	3.68	6.51	7±4	14.78	7.65	13.18	
	Li^8 [d]					4	7.25	3.61	5.75	
	Be^7 [e]	2.5±0.6	6.68	3.02	4.11	11.3±2.8	16.75	7.38	8.75	
In	N^{13} [f]	0.056	0.064	0.020	0.025	0.19	0.116	0.041	0.044	0.27
Au	Li^8 [d]					9	20.10	8.45	10.75	
	Be^7 [e]	1.3±0.3	4.78	1.31	2.07	5.9±1.5	16.22	6.12	6.50	
Pb	He^6 [c]	10±5	13.35	6.11	9.55	21±11	38.30	18.95	29.60	
	N^{13} [f]	0.011	0.042	0.008	0.007	0.11	0.151	0.035	0.028	0.16
U	N^{13} [f]	0.025	0.163	0.030	0.023	0.075	0.550	0.111	0.094	0.125

[a] The calculations were made for the natural isotopic mixture.
[b] Since the calculated cross sections shown in Table II of reference 6 were arrived at by using a slightly different formulation for the emission width, most of the values given there tend to be somewhat lower than the ones shown in this column. When this difference in formulation is corrected for, the systematic shift disappears and the two sets of calculated results are, with one exception, within the stated limits of statistical error. Due to the more accurate formulation of the emission width and the more accurate calculation procedure, the present values are believed to be more accurate ones.
[c] Experimental results of Wolfgang and Rowland[1] for 1.0- and 1.9-Bev proton energy.
[d] Experimental cross sections estimated by Katcoff.[3]
[e] Experimental results of Baker, Friedlander, and Hudis[2] for 1.0- and 2.2-Bev proton energy.
[f] Experimental results of this work for 1.0, 1.9, and 2.9 Bev proton energy.

NaI crystal and the decay of the annihilation radiation was followed. In general the decay curves showed only the 10-min N^{13} activity and background. In some of the earlier runs on zinc, indium, and in almost all runs on lead a small amount of longer-lived activity was also present. The detection efficiency of the counter was determined by means of aliquots of a Sr^{85} solution calibrated by the National Bureau of Standards which were measured under conditions identical to those used in the actual runs. The efficiency of the counter was assumed identical for the 513-kev gamma ray of the Sr^{85} and the 511-kev radiation of N^{13}.

V. EXPERIMENTAL RESULTS

The formation cross sections for N^{13} from zinc, indium, lead, and uranium are given in Table I. Each entry is the average of at least 2 runs unless otherwise indicated. Checks between identical runs at 1.9 and 2.9 Bev were usually within ±10% and at 1 Bev were usually within ±25%. It was necessary to prove that the observed N^{13} activity resulted from the interaction of high-energy protons with the target material and not with a possible impurity. Oxide contamination of the target foils is the most probable contaminant which could lead to spurious experimental results. Oxygen analyses were performed on the zinc and indium foils. The oxygen contamination was low enough and the N^{13} cross sections high enough that no correction had to be made to the observed results. No accurate estimate of the oxygen content could be made for the lead and uranium foils and although the foils were pickled just prior to irradiation it was thought that at least in the 1-Bev irradiations a large fraction of the observed N^{13} activity might be due to the oxygen impurity. However, the formation of N^{13} from targets as heavy as lead and uranium is definitely a high energy phenomenon as can be seen from Table I, where the experimental N^{13} formation cross sections rise by a factor of 10 to 20 between 1 and 3 Bev. One would expect therefore that at still lower energies the N^{13} yields would be too small to measure. Lead and uranium were both irradiated with 400-Mev protons and apparent N^{13} formation cross sections of 0.007 mb for Pb and 0.015 mb for U were observed. It is believed that these cross sections are due almost entirely to oxygen. Since the cross section for the production of N^{13} from O^{16} is essentially constant between 400 and 5700 Mev,[9,10] since the foils were from the same stock of lead and uranium that was irradiated at the higher energies, and since the foils were treated in exactly the same way before the irradiation, the N^{13} cross section at 400 Mev was subtracted from the results at 1.0, 1.9, and 2.9 Bev. The resulting N^{13} formation cross sections at 1.0, 1.9, and 2.9 Bev are plotted as a function of target mass in Fig. 2 and are shown together with the calculated values in Table I.

VI. CALCULATION

The Monte Carlo procedure for heavy particles described previously[11] was used in calculating the emission cross section of N^{13}. The probability of emitting a heavy particle relative to that of emitting a neutron

[9] J. L. Symonds, J. Warren, and J. D. Young, Proc. Phys. Soc. (London), **A70**, 824 (1957).
[10] P. A. Benioff, Phys. Rev. **119**, 316 (1960).
[11] I. Dostrovsky, P. Rabinowitz, and R. Bivins, Phys. Rev. **111**, 1659 (1958).

is given by

$$\frac{P_j}{P_n}=\frac{g_j}{g_n}\frac{(A_j^{\frac{1}{3}}+A_r^{\frac{1}{3}})^2}{(A-1)^{\frac{2}{3}}}\frac{A_jA_r}{A-1}\frac{a_n}{a_j}\frac{R_j}{R_n}\times\exp[2(a_jR_j)^{\frac{1}{2}}-2(a_nR_n)^{\frac{1}{2}}], \quad (1)$$

where $g_j=2I_j+1$ is the number of spin states of the emitted particle. A, A_r, and A_j are the mass numbers of the compound nucleus, the residual nucleus, and the emitted particle, respectively, and

$$R_j=E-Q_j-V_j. \quad (2)$$

Here E is the excitation energy of the compound nucleus, Q_j is the binding energy of particle j, and V_j the Coulomb barrier corrected for penetration. The atomic mass data used in computing the Q values were taken from the compilation of Ashly and Etron.[12]

In Eq. (1), a_j and a_n are the level density parameters which, apart from small corrections [see Eq. (6) of reference 11], are given by

$$a_j=cA_r \quad \text{and} \quad a_n=c(A-1), \quad (3)$$

where c is a constant. This constant was taken in this paper to be $c=0.1$.

Hence Eq. (1) reduces to

$$\frac{P_j}{P_n}=\frac{g_jA_j}{g_n}\frac{(A_j^{\frac{1}{3}}+A_r^{\frac{1}{3}})^2}{(A-1)^{\frac{2}{3}}}\frac{R_j}{R_n}\times\exp[2(a_jR_j)^{\frac{1}{2}}-2(a_nR_n)^{\frac{1}{2}}]. \quad (1a)$$

This equation differs from Eq. (3) of reference 11 in that it takes into account the differences in the geometrical capture cross sections of the heavy particle and the neutron. The geometrical capture cross section is assumed to be $\sigma_g=\pi r_0^2A^{\frac{2}{3}}$ for nucleons bombarding the target nucleus A, and $\sigma_g=\pi r_0^2(A^{\frac{1}{3}}+A_j^{\frac{1}{3}})^2$ for heavier particles. Equation (1a) was used rather than the more accurate equations of Dostrovsky *et al.*[13] since for the excitation energies which are of interest in this paper the additional terms of these equations are negligible.

The competition of fission with the evaporation process was allowed in all calculations but of course is of importance only for U. The expression for the fission width used is that given by Eq. (3) of Dostrovsky *et al.*[14] with the parameters E_S and $(Z^2/A)_{cr}$ of the fission barrier [Eqs. (4) and (5) of reference 14] taken as 18.5 Mev and 47.2, respectively. Evaporation of heavy particles from the fission fragments was neglected since fission of highly excited nuclei occurs towards the end of the evaporation cascade for the above formulation of the fission process. The emission of heavy particles on the other hand is bound to occur at the early stages of the evaporation cascade, when the excitation energy is still very high. Support for the assumption that heavy particle emission from fission fragments might be neglected comes from the work of Katcoff[3] on the spectra of Li^8 particles emitted from various elements. This author found that the Coulomb barrier associated with the spectrum of Li^8 particles emitted from U targets when bombarded with high-energy protons corresponds to residual nuclei in the mass range of U rather than to the mass range of fission fragments. (If it is assumed[15] that high-energy fission occurs early in the evaporation cascade, the reduced probability of heavy-particle emission due to fission competition is probably compensated by heavy-particle evaporation from the highly excited fission fragments, which must then be postulated.)

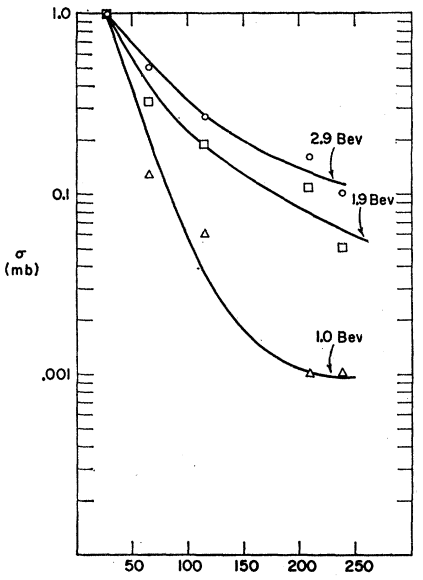

FIG. 2. Experimental N^{13} cross sections as a function of target mass number.

The calculations were applied to the distribution in A, Z, and E of the residual nuclei of the prompt nuclear cascades computed by Metropolis *et al.*[16] Since the targets used in the present work (Zn, In, Pb, U) differ, except for U, from those used in the calculations of Metropolis *et al.* (Cu, Ru, Ce, Bi, U), certain corrections had to be made to the Metropolis A, Z, E distributions. These corrections were applied by shifting A's and Z's of the prompt-cascade distributions as described

[12] V. J. Ashly and H. C. Etron, University of California Lawrence Radiation Laboratory Report UCRL-5419, 1959 (unpublished).

[13] I. Dostrovsky, Z. Fraenkel, and G. Friedlander, Phys. Rev. **116**, 683 (1959).

[14] I. Dostrovsky, Z. Fraenkel and P. Rabinowitz, *Proceedings of the Second United Nations International Conference on the Peaceful Uses of Atomic Energy, Geneva, 1958* (United Nations, New York, 1958), Vol. 15, p. 301.

[15] L. Marquez, Nuovo cimento **2**, 288 (1954); **5**, 6 (1957); **5**, 1646 (1957); Proc. Phys. Soc. (London) **A70**, 546 (1957).

[16] N. Metropolis, R. Bivins, M. Storm, J. M. Miller, G. Friedlander, and A. Turkevich, Phys. Rev. **110**, 204 (1958).

previously.[6] In addition the excitation energies E were adjusted by multiplying each value by a factor (constant for each target and bombarding energy) chosen so as to bring the *average* excitation energy of the prompt-cascade products to the value estimated for the actual target nucleus. This factor was obtained by a linear interpolation between the average excitation energies of the nearest target nuclei given by Metropolis *et al.* Thus, for example, in calculating the cross section from In^{115}bombarded by 1.84-Bev protons, all the excitation energies of the A, Z, E distribution of Ru^{100} bombarded by 1.84-Bev protons as calculated by Metropolis *et al.* were multiplied by 1.080 so as to bring the average excitation energy of the shifted distribution to 270 Mev. This value was obtained by linear interpolation of the average excitation calculated for the prompt cascade products of Ru^{100} and Ce^{140} at 1.84-Bev proton energy. The reliability of this procedure was tested by computing the He^6 and N^{13} emission cross sections of In^{115} bombarded with 1.84-Bev protons using a shifted Ce^{140} distribution and comparing the results with those obtained using the shifted Ru^{100} distribution. The differences for both He^6 and N^{13} were within the statistical errors.

VII. STATISTICS

The small cross section for the emission of N^{13} particles would require inordinately long computer time in order to accumulate reasonable statistics if the regular Monte Carlo procedure was followed. Therefore, an adaptation of the method described by Hudis and Miller[5] was used in calculating the N^{13} emission cross section.

The N^{13} emission cross section from a starting nucleus A_0 with excitation energy E_0 is given by

$$\sigma(N^{13})=\sigma_0(A_0,E_0)\sum_{ij} p(A_i,E_j)P(N^{13};A_i,E_j), \quad (4)$$

where $\sigma_0(A_0,E_0)$ is the formation cross section of the starting nucleus A_0 with excitation energy E_0, $p(A_i,E_j)$ is the probability of formation, somewhere along the evaporation path, of the nucleus A_i with the excitation energy E_j. (For sake of simplicity we assume that A_i has a finite number of possible excitation states, i.e., a discrete rather than a continuous excitation energy spectrum.) $P(N^{13};A_i,E_j)$ is the probability of emitting a N^{13} particle from the state (A_i,E_j). The sum is taken over all excitation energy states E_j and over all possible A_i.

It is, however, the basic assumption underlying the Monte Carlo procedure that *on the average* the number $m(A_i,E_j)$ of cascades leading from (A_0,E_0) to the state (A_i,E_j) is given by

$$m(A_i,E_j)=np(A_i,E_j), \quad (5)$$

where n is the *total* number of cascades calculated from the starting nucleus (A_0,E_0). Hence,

$$\frac{\sigma(N^{13})}{\sigma_0(A_i,E_j)}=\frac{1}{n}\sum_{ij} m(A_i,E_j)P(N^{13};A_i,E_j). \quad (6)$$

The right-hand expression is equivalent to summing the partial N^{13} emission probabilities over all stages of the n evaporation cascades and dividing by n. Obviously similar expressions hold for all other particles emitted.

The regular Monte Carlo procedure as described previously[11] was followed. However the N^{13} emission cross section was not obtained from the number of N^{13} particles emitted in the cascades, but by summing the N^{13} emission probabilities over all steps of the cascade and over all cascades.

Ten evaporation cascades were computed for each member of the A, Z, E distribution of Metropolis *et al.*[16] The accuracy of the emission probability computed by the above procedure is limited only by the statistical variations of the evaporation path and *not* by the magnitude of the probability itself. The standard deviations of the emission probabilities of N^{13} and Be^7 due to the path variations were estimated by computing 20 means of groups of 10 cascades, all starting from the same excited nucleus. Means of 10 cascades were taken rather than individual cascades since in the actual calculation 10 cascades are computed for each starting nucleus. This procedure was therefore adopted as the more appropriate one. This calculation was performed on two representative starting nuclei, Rh^{104} at 135-Mev excitation energy and Te^{98} excited to 330 Mev. The standard deviations for N^{13} were 12.0% and 7.6%, respectively, while for Be^7 the equivalent numbers were 8.5% and 4.2%. The larger standard deviation of the N^{13} emission probability is due to the greater excitation energy dependence of its evaporation probability. Only the first few steps in the evaporation cascade contribute substantially to its emission probability and the smaller number of these steps as compared to Be^7 leads to a higher variance. On this basis we estimate that the standard deviation of the computed N^{13} cross sections is approximately 10% and for the other more abundant heavy particles, He^6, Li^8, and Be^7, it is approximately 5%.

VIII. CALCULATED RESULTS AND DISCUSSION

The calculated cross sections for N^{13} using three different formulations for the interaction radius are shown together with the experimental results in Table I. Also shown in this table are calculated and experimental results for the emission cross sections of He^6, Li^8, and Be^7. The calculated values were recomputed using the modified Monte Carlo procedure described in this paper. The experimental cross sections were measured for proton bombarding energies of 1.0, 1.9, and 2.9 Bev. Since calculated prompt cascade results[16] are available

for proton bombarding energies of 0.94 and 1.84 Bev but not for ~2.9 Bev, the theoretical cross section could be calculated for the former two bombarding energies only.

In studying the A dependence of heavy-particle emission, two factors must be taken into account. As has been shown by Metropolis *et al.*,[16] the average energy deposition for a given proton energy increases with the mass number of the target, this effect becoming more pronounced as the bombarding energy is increased. This would tend to increase the emission cross section of heavy particles with increasing A of the target. On the other hand, the increase in Z and the resulting increase in the Coulomb barrier will obviously tend to decrease the heavy-particle emission width. Looking at the experimental results one observed that for $Z \leq 3$ the first effect seems to predominate whereas for $Z \geq 4$ the Coulomb barrier effect is the stronger one and the cross sections decrease with increasing mass number.

The change in the A dependence for Be^7 was not reproduced in the calculated results of reference 6. Furthermore the calculated values for the He^6, Li^8, and Be^7 cross sections were generally larger than the experimental cross sections and this discrepancy increased with increasing mass of the target. Both these effects might be due to an overestimate of the interaction radius (and hence an underestimate of the Coulomb barrier). In reference 6 the interaction radius was taken to be

$$R=1.5(A_1^{\frac{1}{3}}+A_2^{\frac{1}{3}})\times 10^{-13}\text{ cm}. \quad (7)$$

The examination of the N^{13} cross sections in Table I shows that although the agreement between experimental and calculated values using Eq. (7) is within a factor of approximately 2 (except for U), here again seems to be a systematic difference in the A dependence of the cross sections. Thus the calculated cross sections from Zn are too low by a factor of approximately 2 while those from Pb are too high and for U the discrepancy is a factor of 5. The discrepancy for Be^7, already discussed, is again seen in Table I.

Assuming a nuclear radius of $1.5\ A^{\frac{1}{3}}\times 10^{-13}$ cm, the formulation of the interaction radius as given by Eq. (7) ignores the penetration of the diffuse edge of the nuclei and their distortion at the point of interaction. We have tried to allow for these effects, (a) by subtracting from the above expression of the interaction radius a constant amount (1.2×10^{-13} cm) to give

$$R=[1.5(A_1^{\frac{1}{3}}+A_2^{\frac{1}{3}})-1.2]\times 10^{-13}\text{ cm}; \quad (8)$$

or alternatively, (b) by taking a nuclear radius parameter close to that obtained by electron scattering experiments and adding a constant distance of 2.0×10^{-13} cm for each nucleus, viz.

$$R=[1.1(A_1^{\frac{1}{3}}+A_2^{\frac{1}{3}})+2.0]\times 10^{-13}\text{ cm}. \quad (9)$$

Equation (8) has previously been used by other authors in computing the compound nucleus formation cross sections for α particles[17] and deuterons.[18]

The calculated emission cross sections for He^6, Li^8, Be^7, and N^{13} using the above formulations of the interaction radius are shown together with those obtained using Eq. (7) in Table I. It is seen that the expressions of Eqs. (8) and (9) lead to definite improvement in the agreement between experimental and calculated cross sections for He^6, Li^8, and Be^7 for all targets. However, the agreement of the N^{13} values while improved for U results, is poorer for the other targets. Evidently, if the discrepancy is really due to the inaccurate formulation of the interaction radius, the correct value is given by a more complicated expression.

The calculated results for Zn and Cu targets are open to some doubt due to the fact that the statistical model cannot be assumed to be strictly applicable in the light-element region. However, for these target elements the light-element region is reached only towards the end of the cascade where heavy-particle emission is unlikely. The uncertainty of the results due to the above considerations is hence probably quite small.

Another factor which should be taken into account in comparing the experimental N^{13} cross sections from Zn with the calculated values, is the possibility that at least a part of the experimental N^{13} cross section is due to the formation of this nuclide as the *residual nucleus* of the cascade rather than through evaporation. (Due to the much higher emission cross sections of He^6, Li^8, and Be^7 and also due to the somewhat longer evaporation cascade necessary to form these nuclides as residual nuclei, this effect is negligible for these lighter particles.) In view of the inherent inaccuracy of calculations based on the statistical model in the light-element region, no effort was made to obtain an accurate calculated value for the formation cross section of N^{13} as a residual nucleus. Such a calculation would also have taken an inordinately large amount of computer time since the statistical accuracy would not have been improved by following the modified Monte Carlo procedure, which was used for the computation of the emission probability. However a rough estimate suggests that the residual N^{13} nuclei may account for the bulk of the experimental cross sections at 1.9 Bev for the Zn target.

The heavy particle emission cross sections are very sensitive to relatively small changes of a, the level density parameter. Calculations have shown that changing a from $a=A/10$ to $a=A/12.5$ affect the cross sections in a way similar to changing the interaction radius from Eq. (8) to Eq. (7). It follows that in the absence of a more precise knowledge of the level density parameter and its dependence on A and possibly on E, it is impossible to determine the interaction

[17] J. Blatt and V. F. Weisskopf, *Theoretical Nuclear Physics* (John Wiley & Sons, Inc., New York, 1952), Chap. 8.
[18] M. M. Shapiro, Phys. Rev. **90**, 171 (1953).

radius in heavy-particle interactions to a greater precision from experiments such as those discussed here. Our results can thus not be interpreted as a definite proof that the experimentally observed N^{13} cross sections are due to an evaporation mechanism. Other mechanisms, such as fragmentation, cannot be excluded on the basis of our results. It is, however, clear that the statistical model may well be able to explain all the experimentally observed cross sections of heavy-particle formation, though a more accurate formulation of some of the parameters of the model is obviously required for obtaining a better fit with experimental results.

ACKNOWLEDGMENTS

This work was partly done while one of the authors (I.D.) was a guest at the Chemistry Department, Brookhaven National Laboratory. He wishes to express his appreciation of the hospitality accorded to him.

The authors wish to thank Dr. G. Friedlander and Professor J. M. Miller for many fruitful discussions.

APPENDIX

Details of target solutions:

Zn dissolved in $6N$ HCl(Fe^{++}) plus $PtCl_4$ solution;
In dissolved in $12N$ HCl(Fe^{++}) plus $PtCl_4$ solution;
Pb dissolved in HBr, 48% (Fe^{++}) plus $PtCl_4$ solution;
U dissolved in $6N$ HCl.

The HCl and HBr were treated with iron wire just prior to use to insure the presence of Fe^{++}, which was considered helpful in preventing oxidation of reduced forms of nitrogen.

The addition of $PtCl_4$ to the acid is very helpful in reducing the time required to dissolve the target foils.

It was observed that the presence of water greatly reduced the speed with which the lead foils could be dissolved. In this case the desired amount of NH_4OH carrier solution was added to a few ml of HBr and the solution was boiled until HBr fumes were observed.